Design principles of collateral sensitivity-based dosing strategies

Linda B. S. Aulin[1*], Apostolos Liakopoulos[2], Piet H. van der Graaf[1,3], Daniel E. Rozen[2], J. G. Coen van Hasselt[1*]

1. Leiden Academic Centre for Drug Research, Leiden University, Leiden, The Netherlands

2. Institute of Biology, Leiden University, Leiden, The Netherlands

3. Certara, Canterburry, United Kingdom

*Corresponding authors:

Linda Aulin, l.b.s.aulin@lacdr.leidenuniv.nl, Leiden University, Einsteinweg 55, 2333 CC, Leiden, The Netherlands

Coen van Hasselt, coen.vanhasselt@lacdr.leidenuniv.nl, Leiden University, Einsteinweg 55, 2333 CC, Leiden, The Netherlands

Abstract:	150/150
Manuscript incl Method section:	5058/5000
Figures:	10
Tables:	0
References:	39
Supplemental material:	5 Figures, 1 Table

Keywords: collateral sensitivity, pharmacodynamics, antimicrobial resistance

Abstract

Collateral sensitivity (CS)-based antibiotic treatments, where increased resistance to one antibiotic leads to increased sensitivity to a second antibiotic, may have the potential to limit emergence of antibiotic resistance. However, it remains unclear how to best design CS-based treatment schedules. To address this problem, we use mathematical modelling to study the effects of pathogen- and drug-specific characteristics for different treatment designs on bacterial population dynamics and resistance evolution. First, we confirm that simultaneous or one-day cycling treatment schedules were most effective to supress resistance. Next, we show that the efficacy of CS-based cycling therapies depends critically on the order of drug administration. Finally, we find that reciprocal CS is not essential to suppress resistance, a result that significantly broadens treatment options given the ubiquity of one-way CS in pathogens. Overall, our analyses identify key design principles of CS-based treatment strategies and provide guidance to develop treatment schedules to suppress resistance.

Funding

This work is funded by ZonMW Off Road (Project number 451001033) and NWA Idea Generator (Project number NWA.1228.192.140). AL and DER were supported through the JPI-EC-AMR (Project 547001002).

43 # Introduction

44 Antimicrobial resistance (AMR) is a worldwide health threat due to the reduction of clinically effective antibiotics.
45 Current drug discovery pipelines of new-in-class antibiotic agents are insufficient to offset the emergence of new
46 AMR[1]. Innovative strategies to reduce the rate that AMR develops are thus critically needed. Treatment with
47 antibiotics in individual patients represents one important situation where *de novo* AMR may emerge[2,3]. However,
48 antibiotic dosing strategies used in the clinic do not typically explicitly consider within-host emergence of AMR.
49 Instead, current clinical strategies are primarily based on exposure targets that are associated with sufficient
50 bacterial kill in preclinical studies, or with clinical outcomes in patient studies[4]. Thus, there is need for clinical dosing
51 strategies designed to suppress emergence of AMR[5].

52 Selection inversion mechanisms that exploit evolutionary trade-offs associated with AMR are of increasing interest
53 to design antibiotic dosing strategies that suppress the within-host emergence of AMR [6]. In this context, collateral
54 sensitivity (CS), where resistance to one antibiotic leads to increased sensitivity to a second antibiotic, has been
55 proposed as a potential strategy to suppress AMR [7,8]. CS has been extensively characterized *in vitro*, typically by
56 evolving AMR strains and then quantifying correlated changes in the sensitivity to other antibiotics[9–12]. CS effects
57 have been characterized for several clinically relevant pathogens, including *Escherichia coli*[9,13], *Pseudomonas*
58 *aeruginosa*[14], *Enterococcus faecalis*[13], *Streptococcus pneumoniae*[15], and *Staphylococcus aureus*[16]. CS relationships
59 between antibiotics can either be one directional, where decreased sensitivity to one antibiotic show CS to a second
60 antibiotic but not the reverse, or reciprocal, where decreased sensitivity either of the antibiotics results in CS to the
61 other. Reciprocal CS is often considered a prerequisite for effective CS-based treatments, but such relationships have
62 been less frequently observed compared to one directional CS[9–16].

63 CS-based treatment strategies can use different designs to combine antibiotics showing a CS-relationship, including
64 simultaneous, sequential, or cyclic (alternating) administration. For example, consider a cycling drug strategy using
65 two antibiotics showing reciprocal CS (**Figure 1**). Initial treatment would start with antibiotic A. This leads to
66 resistance to A and a corresponding increase in sensitivity to B. When treatment is switched to antibiotic B, the
67 inverted selection pressure leads to the eradication of cells that are resistant to antibiotic A (due to CS), but possibly
68 favouring any remaining cells that are resistant to B, but susceptible to antibiotic A. . By cycling between the two
69 drugs to sequentially eliminate all cells that show reciprocal CS, complete eradication can been achieved. Although

70 the conceptual strategies of CS-based treatments have been discussed[6], it remains unclear when CS-based dosing
71 strategies are most likely to be beneficial, and how to design specific antibiotic dosing (combination) schedules
72 based on CS. Furthermore, it is unclear how pathogen-specific factors, such as CS effect magnitude and
73 directionality, fitness costs of resistance, and mutation rates, as well as pharmacological factors related to
74 pharmacokinetics (PK) and pharmacodynamics (PD) for different drug types, can affect optimal dosing schedules.

75 Experimental studies *in vitro* are essential to characterize the incidence, evolvability and magnitude of CS, all of
76 which are important but isolated components that may contribute to the success of CS-based treatments [9–16].
77 However, for translation of *in vitro* CS findings to *in vivo* or clinical treatment scenarios, consideration of
78 pharmacodynamic (PD) and pharmacokinetic (PK) factors is essential, as these determine the differential impact of
79 different antibiotics on the rate and concentration dependent effects of bacterial growth, inhibition, and killing [17,18].
80 By affecting bacterial dynamics, antibiotic PK-PD can have a profound influence on resistance evolution, and are
81 therefore key factors to design optimised CS-informed treatments. To this end, mathematical models are important
82 tools to integrate multiple biological and pharmacological factors contributing to treatment outcomes, including
83 different PK parameters of specific antibiotics in patients, antibiotic-specific PD parameters, and pathogen specific
84 characteristics such as strain fitness and the rate and magnitude of CS effects. Thus, using a mathematical modelling
85 approach allows the addressing of key questions relating to CS-based treatments that cannot be easily s
86 experimentally.

87 In the current study we aim to determine if and when CS-based dosing schedules are likely to lead to the suppression
88 of within-host emergence of antibiotic resistance. We utilise a mathematical modelling approach to
89 comprehensively study the influence of key pathogen-specific factors and the contribution of PK and PD properties
90 to identify key design principles to inform rational design of antibiotic combination dosing schedules that suppress
91 antibiotic resistance.

92

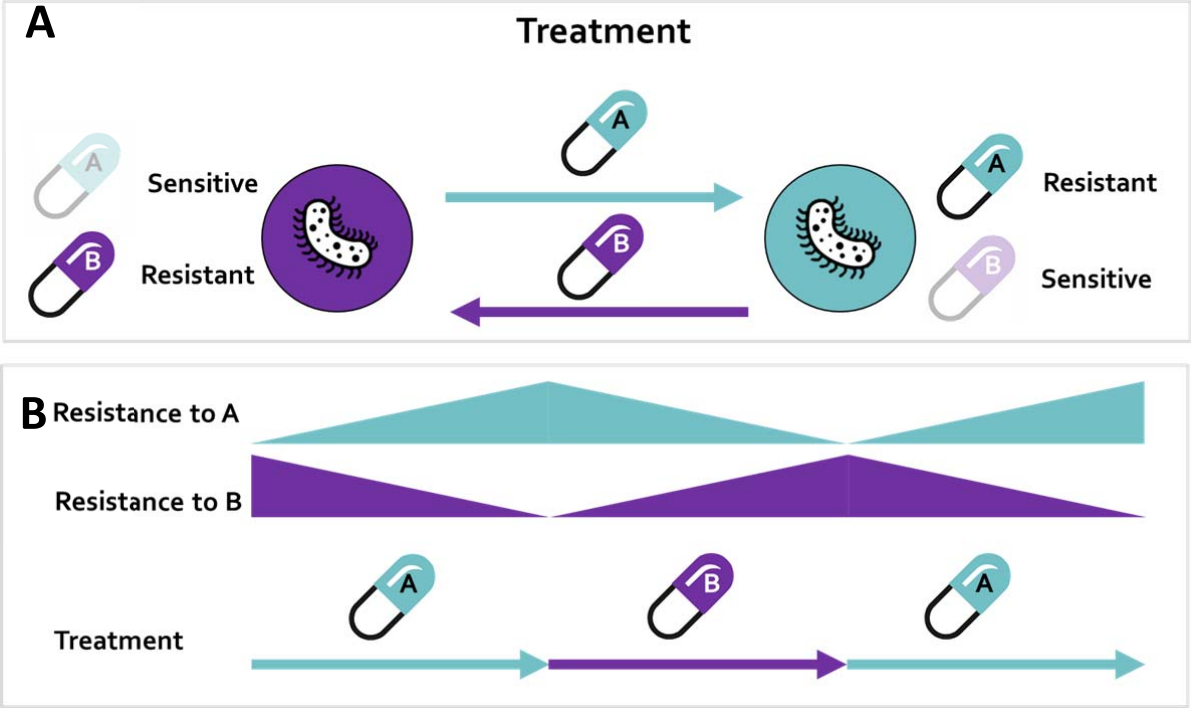

Figure 1. Concept of collateral sensitivity (CS)-based treatments using two hypothetical drugs, antibiotic A and B. Adapted from Pál et al 2015 [39] **A:** Reciprocal CS relationship between antibiotic A and B. **B:** Theoretical cycling regimen exploiting CS between antibiotic A and B to supress resistance.

Methods

Model framework

A differential-equation based model of components accounting for antibiotic PK and PD, and associated bacterial population dynamics, to study the impact of differences in pathogen- and drug-specific characteristics for different treatment strategies for treatment with two antibiotics (AB) referred to as antibiotic A (AB_A) and antibiotic B (AB_B).

Pharmacokinetics

A mono-exponential PK model was defined for both antibiotics AB_i, where i = {A,B}, as follows:

$$\frac{dA_{AB_i}}{dt} = -k_{e,AB_i} \times A_{AB_i} \quad (1)$$

$$t_{half,AB_i} = \frac{ln(2)}{k_{e,AB_i}} \quad (2)$$

$$C_{AB_i} = \frac{A_{AB_i}}{V_{AB_i}} \quad (3)$$

where **Equation 1** describes the change of the amount of AB_i over time after intravenous administration, k_{e,AB_i} is the elimination rate of AB_i, which can also be expressed as a half-life (t_{half,AB_i}) (**Equation 2**). The plasma concentration (C_{AB_i}), which is the assumed driver of the antibiotic effect, is calculated using the V_{AB_i}, the distribution volume of AB_i (**Equation 3**).

Bacterial subpopulations

A model for antibiotic sensitive and resistant subpopulations was defined, comprising of a four-state stochastic hybrid ordinary differential equation (ODE) model, where each state represents a bacterial subpopulation with different antibiotic susceptibility towards AB_A and AB_B.

The model included an antibiotic sensitive bacterial subpopulation (WT) (**Equation 4**), one mutant subpopulation resistant to AB_A but sensitive to AB_B (R_A) (**Equation 5**), one mutant subpopulation sensitive to AB_A but resistant to AB_B (R_B) (**Equation 6**), and one double mutant subpopulation resistant to both AB_A and AB_B (R_{AB}) (**Equation 7**). The initial bacterial population was assumed to be homogeneous and in the sensitive WT state unless stated otherwise.

$$\frac{dWT}{dt} = WT \times k_{net,WT}(WT, R_A, R_B, R_{AB}, k_{Gmax,WT}) \times E_{AB,WT}(E_{AB_A,WT}, E_{AB_B,WT}) - k_{WT,R_A}(WT, \mu) - k_{WT,R_B}(WT, \mu) \quad (4)$$

$$\frac{dR_A}{dt} = R_A \times k_{net,R_A}(WT, R_A, R_B, R_{AB}, k_{Gmax,R_A}) \times E_{AB,R_A}(E_{AB_A,R_A}, E_{AB_B,R_A}) + k_{WT,R_A}(WT, \mu) - k_{R_A,R_{AB}}(R_A, \mu) \quad (5)$$

$$\frac{dR_B}{dt} = R_B \times k_{net,R_B}(WT, R_A, R_B, R_{AB}, k_{Gmax,R_B}) \times E_{AB,R_B}(E_{AB_A,R_B}, E_{AB_B,R_B}) + k_{WT,R_B}(WT, \mu) - k_{R_B,R_{AB}}(R_B, \mu) \quad (6)$$

$$\frac{dR_{AB}}{dt} = R_{AB} \times k_{net,R_{AB}}(WT, R_A, R_B, R_{AB}, k_{Gmax,R_{AB}}) \times E_{AB,R_{AB}}(E_{AB_A,R_{AB}}, E_{AB_B,R_{AB}}) + k_{R_A,R_{AB}}(R_A, \mu) + k_{R_B,R_{AB}}(R_B, \mu) \quad (7)$$

The above equations (**Equation 4-7**) describe the subpopulation specific rate of change for bacterial density, which is dependent on the bacterial density of subpopulation *z*, subpopulation specific net growth ($k_{net,z}$), antibiotic effect ($E_{AB,z}$), and mutation transition(s) ($k_{z,M}$), if present.

Resistance mutation

Resistance evolution was included as stochastic mutation process. This process was modelled using a binomial distribution *B* with a mutation probability equal to the mutation rate (μ). The number of bacteria mutated per time step $k_{z,M}$ depende on the number of bacteria available for mutation (n_z), *i.e.* the bacterial subpopulation density of

subpopulation z multiplied by the infection volume V, for mutation at time t (**Equation 8**). Double resistant mutants evolved through two mutation steps.

$$k_{z,M} = \frac{B(n_z,\mu)}{V} \quad (8)$$

Pharmacodynamic effects

Drug effects on bacterial subpopulations (**Equation 4-7**) were assumed to be additive and the total drug effect for each subpopulation z ($E_{AB,z}$), and was implemented as follows (**Equation 9**):

$$E_{AB,z} = 1 - \left(E_{AB_A,z}(C_{AB,A}, G_{min,\,AB_A}, Hill_{AB_A}, MIC_{AB_A,\,z},\ k_{Gmax,z}) + E_{AB_B,z}(C_{AB,B}, G_{min,\,AB_B}, Hill_{AB_B}, MIC_{AB_B,\,z}, k_{Gmax,z})\right) \quad (9)$$

Here, antibiotic-mediated effects were implemented according to a previously developed PD model [17], where the effect of the ith antibiotic on bacterial subpopulation z ($E_{AB_i,z}$) related to the unbound antibiotic concentration ($C_{AB,i}$) according to Equation 10.

$$E_{AB_i,z} = \frac{(1-G_{min,\,AB_i}/\,k_{Gmax,z})\times\left(\frac{C_{AB,i}}{MIC_{AB_i,\,z}}\right)^{Hill_{AB_i}}}{\left(\frac{C_{AB_i}}{MIC_{AB_i,\,z}}\right)^{Hill_{AB_i}} - \frac{G_{min,\,AB_i}}{k_{Gmax,z}}} \quad (10)$$

where $G_{min,\,AB_i}$ represents the maximal killing effect for the AB_i, $k_{Gmax,z}$ being the subpopulation-specific maximal growth rate, $Hill_{AB_i}$ being the shape factor of the concentration-effect relationship, and $MIC_{AB_i,\,z}$ being the subpopulation-specific MIC of AB_i.

Sensitive bacteria were defined as having a MIC of 1 mg/L (MIC_{WT}) and resistant as 10 mg/L (MIC_R). Because the antibiotic concentrations are expressed as folds times MIC_{WT}, the absolute value of MIC_{WT} is irreverent. However, the ratio between MIC_{WT} and MIC_R is of relevance. A tenfold increase was chosen to represent a significant increase for a biologically plausible scenario. Resistance-related CS effects were included on the two singly resistant mutants (R_A and R_B), and were implemented as a proportional reduction (CS_A and CS_B) of the sensitive MIC (MIC_{WT}). The subpopulation- and antibiotic-specific MICs are stated below:

$MIC_{AB_A,WT} = MIC_{WT}$ and $MIC_{AB_B,WT} = MIC_{WT}$

$MIC_{AB_A,R_A} = MIC_R$ and $MIC_{AB_B,R_A} = MIC_{WT} \times CS_B$

$MIC_{AB_A,R_B} = MIC_{WT} \times CS_A$ and $MIC_{AB_B,R_B} = MIC_R$

$MIC_{AB_A,R_{AB}} = MIC_R$ and $MIC_{AB_B,R_{AB}} = MIC_R$

155 ***Fitness effects***

156 We considered resistance-associated fitness cost by including a fitness cost factor (F_{fit}), which introduced a fractional
157 reduction of the growth rate (k_G) for each resistance mutation. The net growth rate was implemented according to
158 **Equation 11**.

159 $$k_{net,z} = k_{Gmax,z} \times \left(1 - \frac{WT+R_A+R_B+R_{AB}}{B_{max}}\right) \quad (11)$$

160 $$k_{Gmax,z} = k_G \times F_{fit}^{n,z} \quad (12)$$

161 where $k_{net,z}$ is the subpopulation-specific net growth in the absents of antibiotic, B_{max} is the systems maximal carrying
162 capacity, F_{fit} is the fitness cost factor per mutation, and n_z is the subpopulation specific number of mutations (n_z = 0,
163 1 or 2).

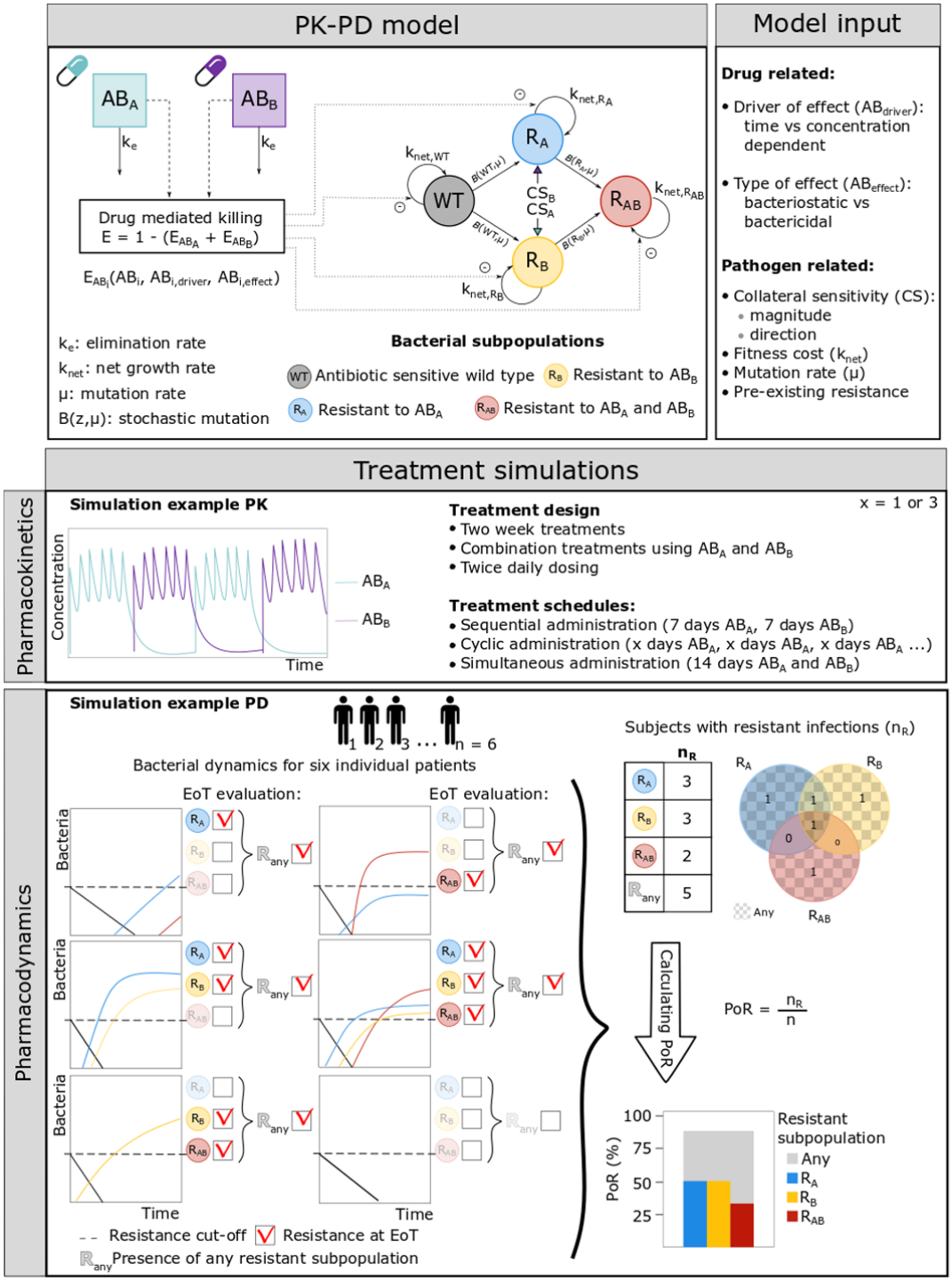

Figure 2. Simulation workflow. Pharmacokinetic-pharmacodynamic (PK-PD) framework comprising of four bacterial subpopulations (WT, R_A, R_B, R_{AB}) and PK-PD of two hypothetical antibiotics (AB_A and AB_B). The framework includes fixed infection- and pathogen-specific parameters and fixed drug PK parameters. The model input includes both drug and pathogen related factors, which vary between different scenarios. The framework was used to simulate different treatment schedules of two week combination treatments using AB_A and AB_B for n patients. In the simulation example a three-day cycling treatment regimen (PK panel) is simulated for six patients. The resulting patient specific bacterial profiles are shown in the PD panel. Resistance was evaluated for each patient and bacterial subpopulation at the end of treatment (EoT), for which the corresponding probability of resistance (PoR) was calculated.

172 ## Pathogen- and infection-specific parameters

173 The maximal growth rate of the hypothetical pathogen was 0.7 h^{-1}, thus representing a doubling time of one hour.
174 The infection-specific parameters were chosen to represent a human bacteraemia, thus a typical human blood
175 volume of five litre was used as the infection site volume[19]. An initial bacterial density of 10^4 colony forming units
176 (CFU)/mL was used to represent a severe infection, which reflects an early stage of an established infection[20]. A
177 system carrying capacity limitation (B_{max}) of 10^8 CFU/mL[20] was implemented according to Equation 12. When the
178 maximal carrying capacity is reached, the net growth of the total bacterial population is zero, resulting in a stationary
179 phase. During this phase bacterial replication continues, but is offset by bacterial death at the same rate, thereby
180 still allowing for resistance mutations to occur. Resistance mutation rates of 10^{-6} and 10^{-9} mutations/base pair/hour
181 were chosen to represent a high and a moderate mutation rate scenario, respectively[21].

182 ## Drug-specific parameters

183 The two hypothetical antibiotics used for the simulations (AB_A and AB_B) have identical one-compartmental PK with
184 distribution volumes of one litre, five-hour half-lives (Table 1), and no protein binding. The selected half-life
185 represents antibiotics with clinically relevant short half-lives, thereby rapidly reaching steady-state concentrations
186 with minimal accumulation. The drugs were administrated as intravenous bolus doses twice daily over a treatment
187 duration of two weeks. Several different dosing regimens were simulated including monotherapy, sequential dosing,
188 cycling regimens, and simultaneous dosing. For sequential and cycling treatments AB_A was used as the starting drug.
189 The doses used were obtained by calculating the required dose to achieve appropriate average steady state
190 concentration (C_{ss}) relative to the MIC_{WT}. The lowest dose that gave kill or stasis of the WT bacteria within the 24
191 hours of treatment, but allowed for resistance development during monotherapy, was selected for all dosing
192 regimens except for the simultaneous dosing, for which the dose for the individual antibiotics were reduced by half.
193 Four different PD types were included using different combinations of parameter values of Hill (driver of antibiotic
194 effect) and G_{min} (type of antibiotic effect), and represented 1) time-dependent (Hill = 0.5) or concentration-
195 dependent (Hill = 3) and 2) bacteriostatic (G_{min} = -1) or bactericidal (G_{min} = -3) antibiotics. The corresponding PK-PD
196 relationship of the four different antibiotic types is shown in **Figure 3**.

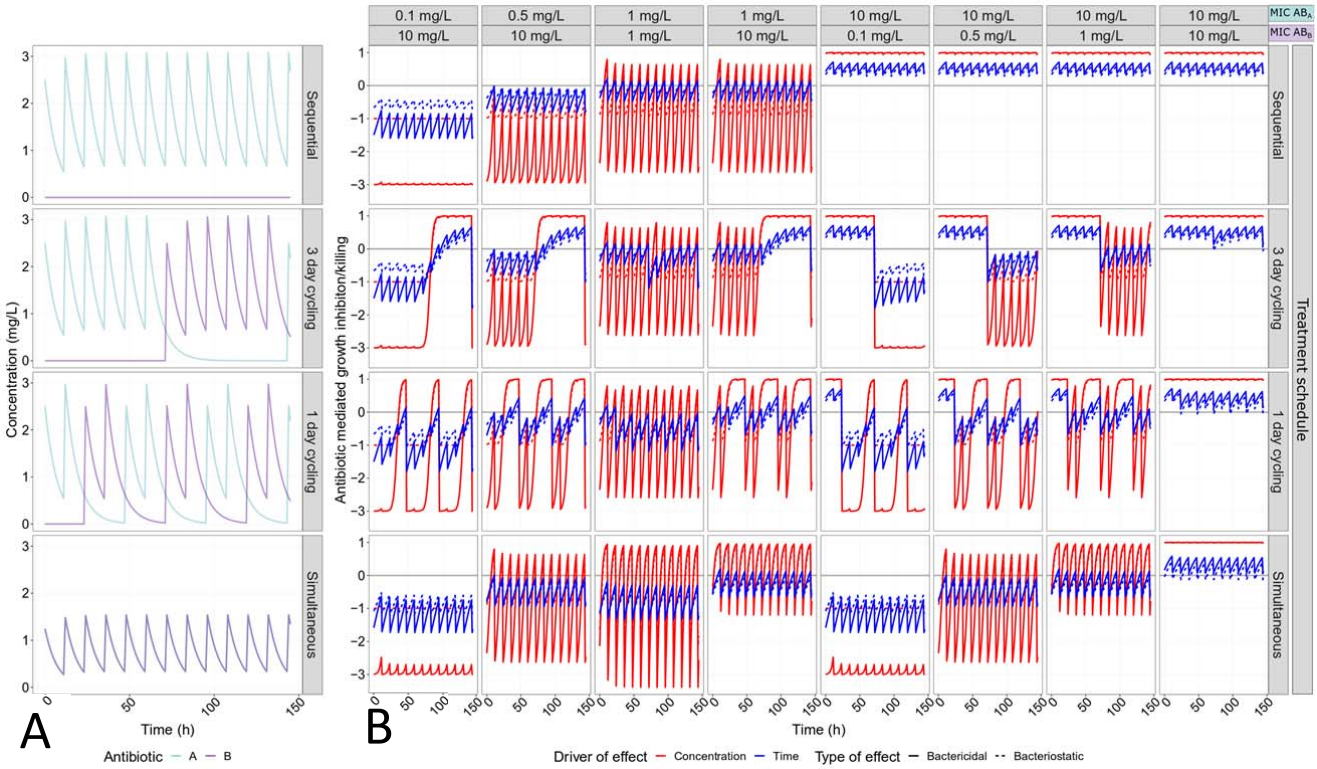

Figure 3. MIC-specific PK-PD relationships. A: Initial pharmacokinetic (PK) profiles of mono or combination treatments using two hypothetical antibiotics AB_A (turquoise) and AB_B (purple), administrated twice daily, with a dose resulting in C_{ss} of 1.5 mg/L or 0.75mg/L for simultaneous dosing. **B**: MIC-specific pharmacodynamic profiles concentration effect relationship of different antibiotic drug types including concentration- (Hill = 3, red) or time- (Hill = 0.5, blue) dependent antibiotics and bactericidal (G_{min} = -3, solid) and bacteriostatic (G_{min} = -1, dashed), where the effect is representing the proportional bacterial growth inhibition/killing. The effect is driven by the PK profile shown in panel A according to Equation 9 and 10.

Simulations scenarios

An initial set of dose finding simulations revealed that monotherapy required C_{ss} equal to 1.5 x MIC_{WT} to achieve killing of the WT, regardless of the drug type used (**Figure S1**). This C_{ss} was subsequently used for treatment scenarios unless explicitly stated otherwise.

We used a systematic simulation strategy to study the impact of CS, fitness cost, initial subpopulation heterogeneity in antibiotic sensitivity, and mutation rate on the probability of resistance (PoR) development for different treatments. An overview of all simulated scenarios can be found in **Table S1**. We simulated treatments using two same-type antibiotics for scenarios without CS as well as in the presence of one directional and reciprocal CS in the magnitude of 50% or 90% reduction of the sensitive MIC (**Table S1**, **Scenario 1** and **2**). For these scenarios the

214 resistance was assumed to occur without any fitness cost, thus allowing us to evaluated CS-specific effect on PoR.
215 We also simulated a set of treatment scenarios using two different antibiotic type in the presence or absence of CS
216 (**Table S1**, **Scenario 3)**. Additionally, we simulated same-type treatment scenarios covering a wide range of fitness
217 costs (10% to 50% per mutation) implemented as a growth rate reduction (**Table S1**, **Scenario 4)**. To assess the
218 impact of therapeutic window of antibiotics, as reflected by the fold-difference of steady state concentration (C_{ss}) to
219 the MIC_{WT}, we simulated different dosing levels resulting in a range of C_{ss} of 0.5-5 x MIC_{WT} (**Table S1**, **Scenario 5)**. In
220 order to better understand the interplay between CS and fitness cost we simulated these scenarios with and without
221 CS. We further investigated how low levels of pre-existing resistance (1%) towards either AB_A or AB_B affected the PoR
222 at the end of treatment for different dosing regimens (**Table S1**, **Scenario 6)**. Finally, we examined the effect of
223 increased mutation rates on resistance development (**Table S1**, **Scenario 7)**.

224 Each simulated scenario was realized 500 times (n), thus representing 500 virtual patients.

225 Evaluation metrics

226 For evaluation of the simulated scenario's we computed the probability of resistance (PoR), which was defined as
227 resistant bacteria reaching at the end of treatment at least the initial bacterial density of 10^4 CFU/mL, for each
228 population separately (Equation 13)

229 $$PoR_z = \frac{n_{R,z}}{n} \quad (13)$$

230 where $n_{R,z}$ denotes the number of patients having resistant bacteria of subpopulation *z* at the end of treatment
231 (Equation 14):

$$n_{R,z} = \sum_{k=1}^{n} \mathbf{1}_{x_{z,k} \geq 10^4 cfu/mL}$$

232 (14)

233 where **1** denotes the indicator function and $x_{z,k}$ denotes the bacterial density of subpopulation *z* at the end of
234 treatment of patient *k*.

235 Furthermore we also calculated the PoR for the case where any, i.e., one or more resistant subpopulation(s)
236 exceeded the resistance cut-off (R_{Any}).

237

238 The standard error (SE) of the PoR was calculated according to **Equation 15**.

239 $$SE = \sqrt{\frac{PoR(1-PoR)}{n}} \quad (15)$$

240 ## Software and model code

241 All analyses were conducted in R version 4.0.5, using the ODE solver package RxODE (version 1.0.0-0)[22,23]. The
242 associated model code is available at https://github.com/vanhasseltlab/CS-PKPD).

243 # Results

244 ## Drug type and treatment schedule influence the probability of resistance

245 We simulated antibiotic combination treatments of two antibiotics from the same type, with either no (0%) or
246 reciprocal CS (50 or 90% decrease of MIC_{WT}). We show that the impact of reciprocal CS on resistance dynamics is
247 dependent on the simulated drug type and dosing regimen (**Figure 4**). Treatments with concentration dependent
248 antibiotics could achieve full CS-based resistance suppression for dosing schedules using one-day cycling interval
249 (**Figure 4C, 4G**) or simultaneous administration (**Figure 4D, 4H**). A 50% MIC reduction was sufficient to achieve this
250 effect for all of the four treatments, which is relevant in light of experimental results consistent with these CS
251 magnitudes. Treatments using time dependent antibiotics dosed according to these schedules (**Figure 4K, 4L, 4O, 4P**)
252 were efficient in fully supressing resistance with or without CS. Full resistance suppression was not achieved by any
253 of the other treatment schedules tested. Although none of the CS-based treatments dosed according to the three-
254 day cycling regimen managed to fully supress resistance, the ones using time dependent antibiotics (**Figure 4J, 4N**)
255 did show reduced PoR in presence of CS. For these treatments, the effect of CS was most prominent for the
256 bacteriostatic antibiotics (**Figure 4N**) where a CS magnitude of 90% resulted in ΔPoR -12.6% for R_{Any}. Such a
257 decreased could have a potential clinical benefit. Importantly, we also find that for some treatments the presence of
258 CS was not only unable to fully supress resistance, but favoured the formation of double resistant mutants (**Figure**
259 **4F, 4I, 4M).**

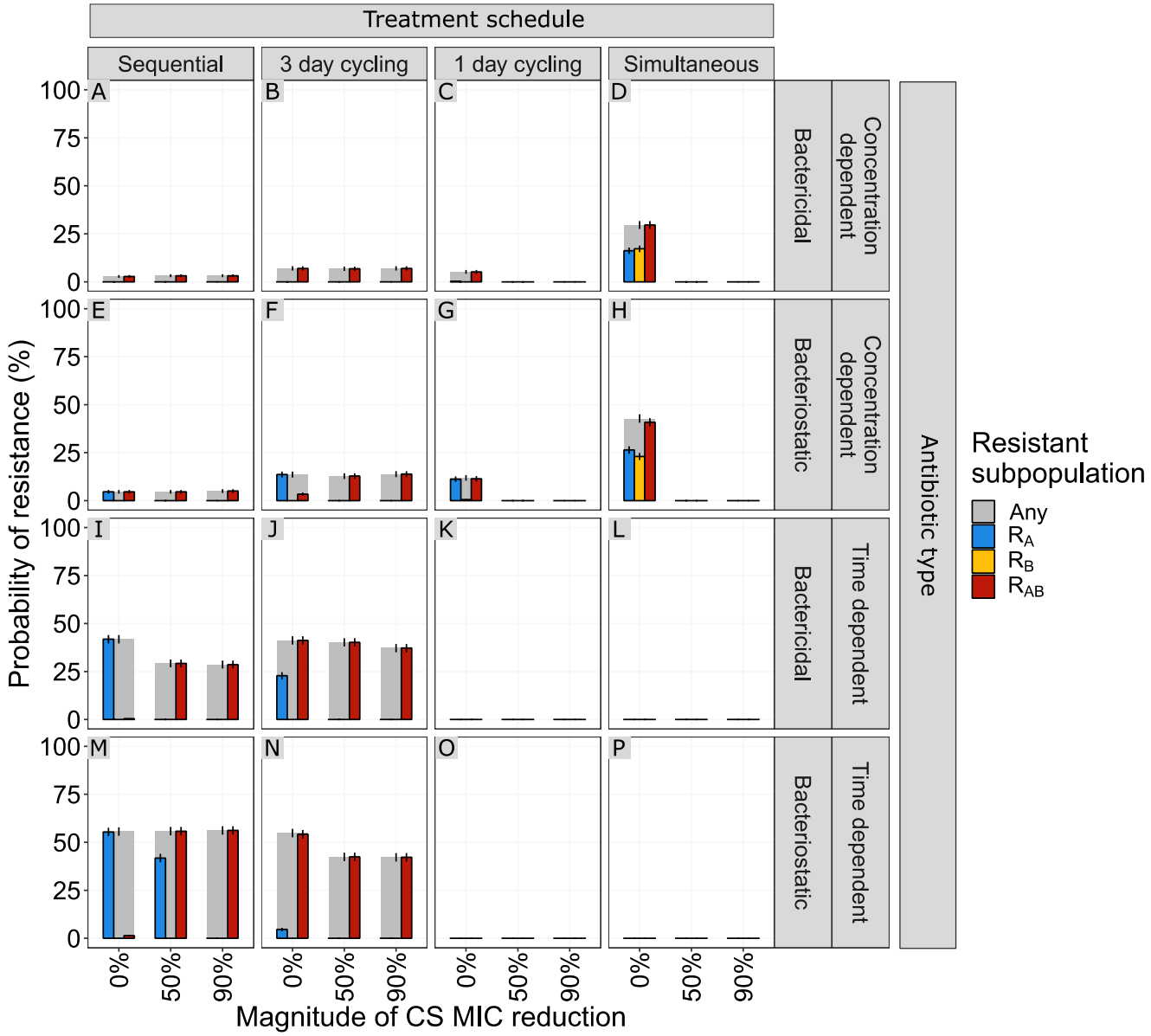

Figure 4. The effect of treatment design and antibiotic in relation to different levels of collateral sensitivity (CS) on the probability of resistance (PoR) at end of treatment. The simulations show that CS had a profound impact on resistance development for treatments with concentration dependent antibiotics with one-day cycling interval or simultaneous administration. PoR was estimated at end of treatment for treatments using different designs (columns) and antibiotic types (rows). Subpopulation-specific PoR are indicated by different colour and R_{Any}, defined as the presence of any resistant subpopulation, is indicated in grey. The error bars represent the standard error of the estimation of PoR.

Directionality of CS effects influence the probability of resistance

We next sought to determine if reciprocity is a requirement for CS-based treatments to suppress *de novo* resistance. We find that bactericidal and bacteriostatic drugs showed the same overall behaviour for the treatment tested when related to CS directionality (**Figure S2**). We specifically focus on the one-day cycling and simultaneous treatment that

271 appeared to be most successful in fully supressing resistance development for reciprocal CS. We find that for the
272 one-day cycling regimen the presence of one directional CS for the second administrated antibiotic (AB_B) is sufficient
273 to fully suppress resistance development. This is illustrated for treatments using concentration dependent
274 bacteriostatic antibiotic in **Figure 5**. In this scenario, one directional CS results in resistance levels close to the
275 reciprocal scenario (*e.g.*, one directional 50% CS resulted in 0.4% PoR of R_{Any} for bacteriostatic (Figure 5A) vs 0% for
276 reciprocal CS (Figure 5B)). In contrast, when CS is only present for the first antibiotic (AB_A) administered, we found
277 resistance levels close to the scenario without any CS (PoR 11.5% (Figure 5D) vs 12.4% (Figure 5C)). Overall, these
278 results suggest that when designing CS-based one-day cycling treatments using a drug-pair without reciprocity, the
279 order for which these are administrated has a large impact on treatment success and the therapy should be initiated
280 with the antibiotic for which there is no CS. This strategy allows for evolution and growth of R_A on the first day, while
281 R_B is supressed by AB_A. When the selection is inverted on day two, the low levels of R_A present is effectively killed by
282 AB_B in the presence of CS. In the absence of CS towards AB_B, R_A will reach high levels, which can lead to further
283 evolution of the R_{AB}. When simultaneous administration of concentration-dependent antibiotics is used, we found
284 that reciprocity is necessary to fully supress resistance, as one directional CS will only supress resistance for the
285 resistant subpopulation which show CS (**Figure 5A and 5B**). However, one directional CS did reduce the PoR for R_{Any}
286 by approximately 50% (ΔPoR -19.6% and -19.2% for CS_A and CS_B, respectively) for both of these treatments, thus
287 having a potential clinical value.

288

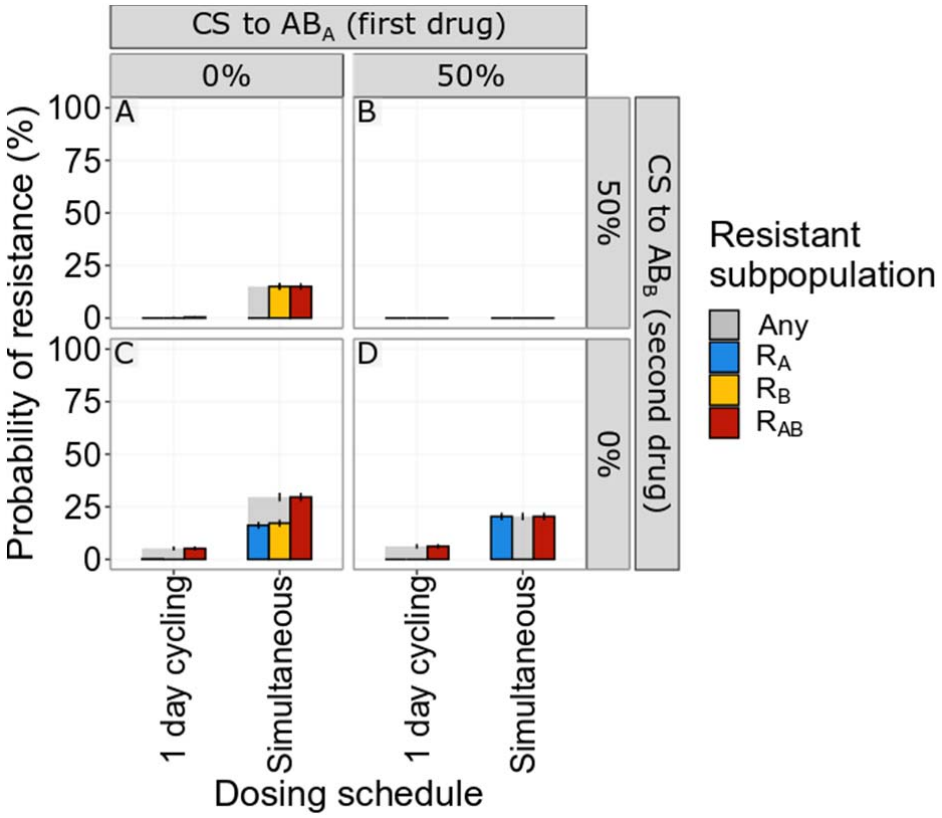

Figure 5. The effect of the direction or reciprocally of collateral sensitivity (CS) on end of treatment probability of resistance (PoR). PoR was estimated at end of treatment for different CS scenarios using concentration dependent bacteriostatic drugs. Subpopulation-specific PoR is indicated by different colour and R_{Any} resistance, defined as the presence of any resistant subpopulation, is indicated in grey. The error bars represent the standard error of the estimation of PoR. For the one-day cycling regimen it became evident that the CS towards the second administrated drug (AB_B) was driving the effect, CS-based dosing using simulations administration of concentration dependent antibiotics showed that reciprocity is necessary to supress overall resistance.

Administration sequence and antibiotic type influence resistance suppression

As CS dose not only occur between antibiotics of the same type, it is important to understand how the administration sequence of different-type antibiotics affect resistance evolution in the presence of reciprocal CS. Our results for one-day cycling and simultaneous schedules demonstrated that the suppression of *de novo* resistance was mainly driven by the first administrated antibiotic (AB_A) for all non-simultaneous regimens (**Figure S3**), highlighting the importance of drug sequence. In line with our findings for same-type antibiotic combination treatments (**Figure 4**), resistance was fully suppressed from CS only when using one-day cycling or simultaneous administration dosing regimens. Particularly for one-day cycling regimens (**Figure 6**), initiating treatment with a time-

305 dependent antibiotic was more effective at supressing resistance in the presence of reciprocal CS compared to the

306 initial administration of a concentration dependent antibiotic.

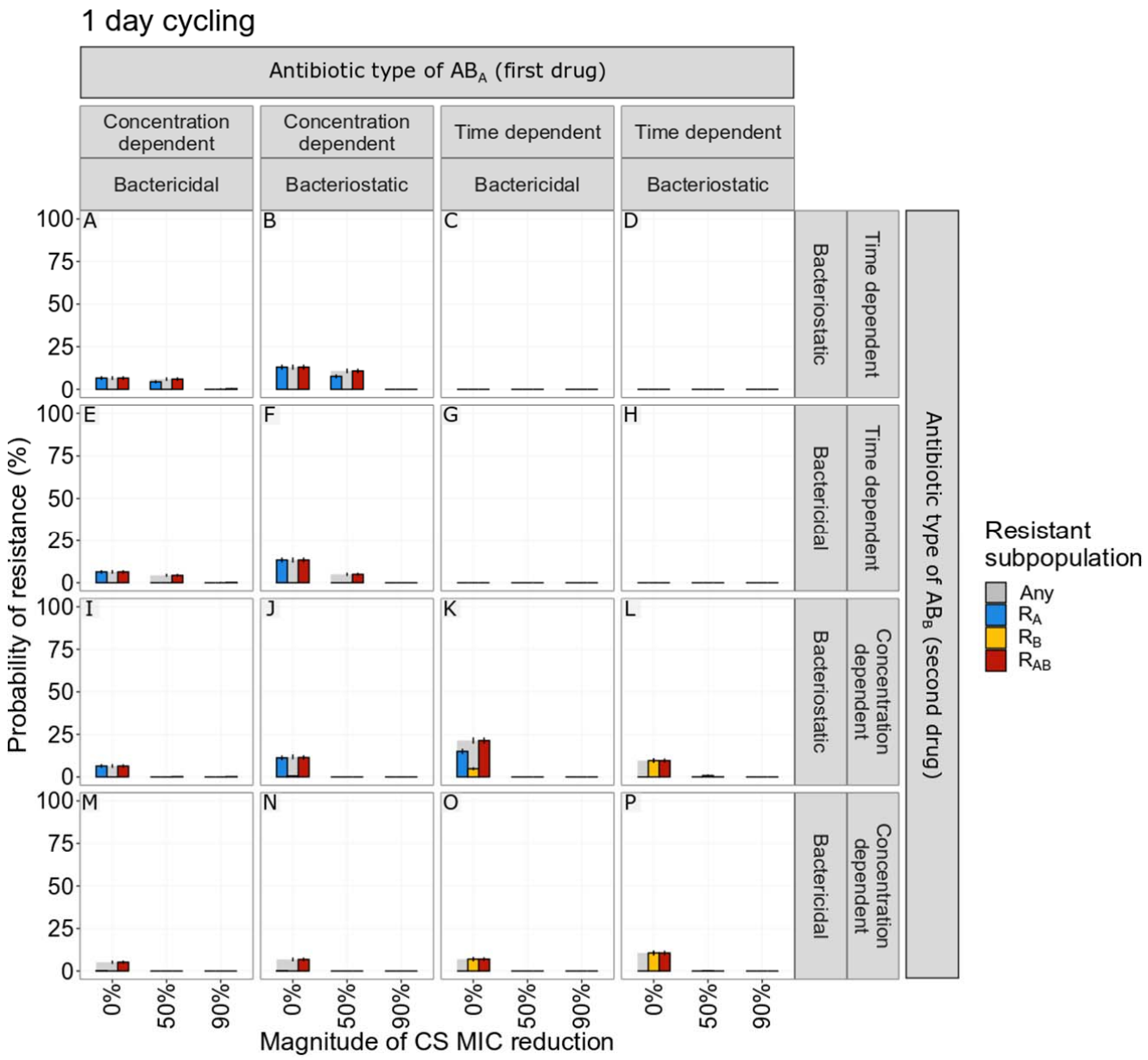

307

308 **Figure 6. The effect of using different antibiotic combinations during one-day cycling treatments in relation to different levels of collateral**

309 **sensitivity (CS) on the probability of resistance (PoR) at the end of treatment.** The simulations showed that initiating treatment with a time

310 dependent than with a concentration dependent antibiotic was more effective in supressing resistance in the presence of reciprocal CS. PoR

311 was estimated at the end of treatment for one-day cycling regimen with different antibiotic combinations. Subpopulation-specific PoR is

312 indicated by different colour and R_{Any}, defined as the presence of any resistant subpopulation, is indicated in grey. The error bars represent the

313 standard error of the estimation of PoR.

314 CS-based combinations show greatest promise for antibiotics with a narrow therapeutic window

315 Although many antibiotics are well-tolerated and can be dosed well above the MIC of susceptible strains others, *e.g.*,
316 aminoglycosides, display a narrow therapeutic window due to toxicity[24–26]. Understanding the relationship between
317 average steady-state concentrations (C_{ss}) and the impact of CS on *de novo* resistance development would help
318 identify which clinical scenarios that CS could be exploited to improve treatment. A set of simulated dosing regimens
319 with same-type antibiotics resulting in C_{ss} between 0.5-5 x MIC_{WT} revealed that CS has the greatest impact on R_{Any} for
320 C_{ss} close to the MIC_{WT} (**Figure 7** and **S4**). Most treatments showing a benefit of CS lost the advantage when the C_{ss}
321 exceeded 1.5 x MIC_{WT}. The only exception was one-day cycling treatment using concertation dependent
322 bacteriostatic drugs, which retained an advantage up to C_{ss} of 2 x MIC_{WT} (**Figure 7G**).

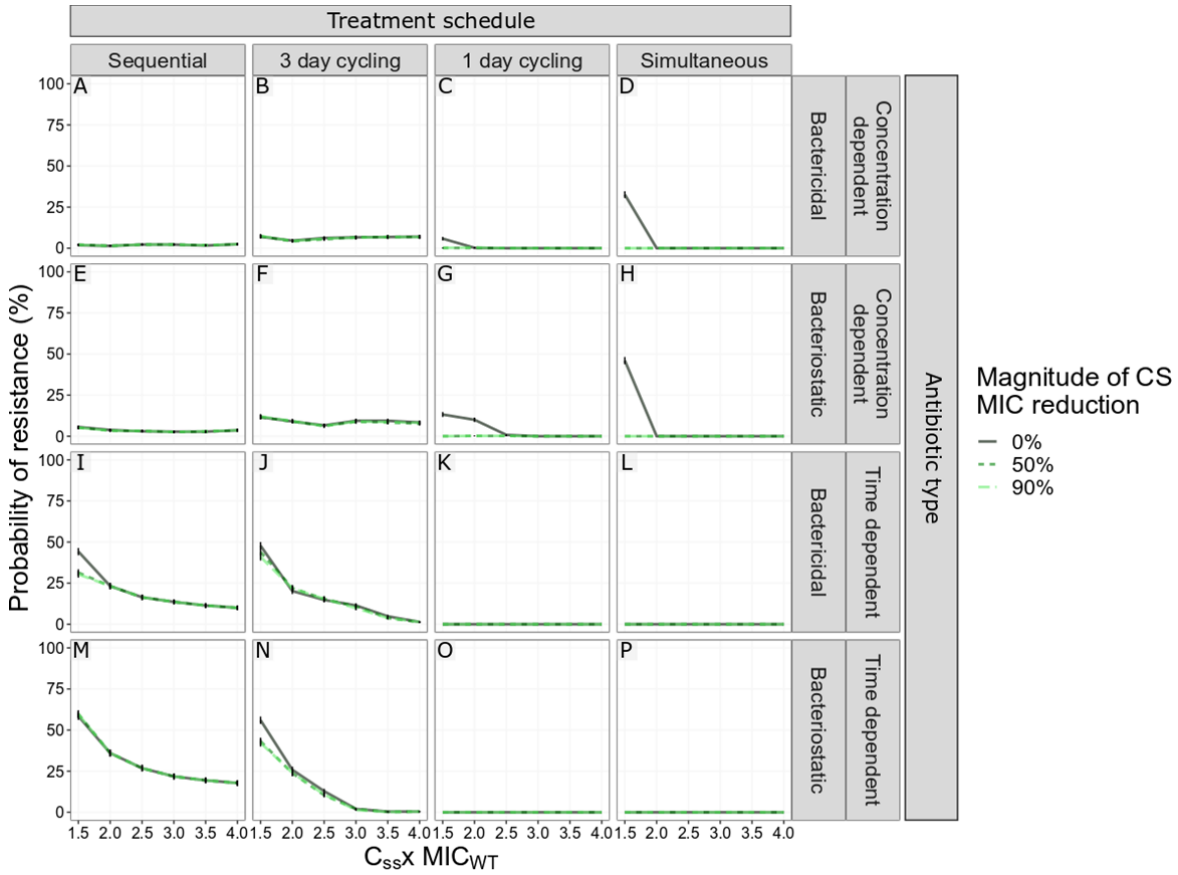

323

324 **Figure 7. The effect of antibiotic steady state concentrations (C_{ss}) in relation to different levels of collateral sensitivity (CS) on the probability**
325 **of resistance at the end of treatment (PoR).** The simulation revealed that CS had the largest impact on PoR for C_{ss} close to MIC of the wild type
326 strain (MIC_{WT}). C_{ss} was expressed as factor difference from the MIC_{WT}. PoR of R_{Any}, defined as the presence of any resistant subpopulation, was
327 estimated at the end of treatment for treatments using different designs (columns) and antibiotic types (rows). Colour and line-type indicate
328 the magnitude of reciprocal CS simulated. The error bars represent the standard error of the estimation.

329

330 ## Fitness cost of antibiotic resistance can contribute to the success of CS-based treatments

331 Resistance evolution is commonly associated with fitness costs.[27]. We studied the impact of different levels of fitness
332 cost on the suppression of *de novo* resistance development (**Figure 8**). Fitness cost was included as a fractional
333 reduction of growth per mutation, thereby doubly penalising the double resistant mutant R_{AB}. In the absence of CS,
334 fitness cost below 50% per mutation had little impact (|ΔPoR| ≥ 5%) on R_{Any} for most treatment scenarios. However,
335 when concentration-dependent bactericidal drugs where dosed simultaneously the presence of fitness costs slightly
336 increased the PoR (maximum ΔPoR 10.2 %). The presence of fitness costs increased the impact of CS on PoR the
337 three-day cycling regimen using time dependent antibiotics (**Figure 8J and 8N**), which failed to fully supress
338 resistance in the presence of fitness cost-free CS. The fitness cost generating the largest impact of CS for these
339 treatments on PoR was 40% and 50% cost per mutation when treated with bacteriostatic (Δ PoR -48.4) and
340 bactericidal (Δ PoR -42.8%) drug, respectively.

341

342

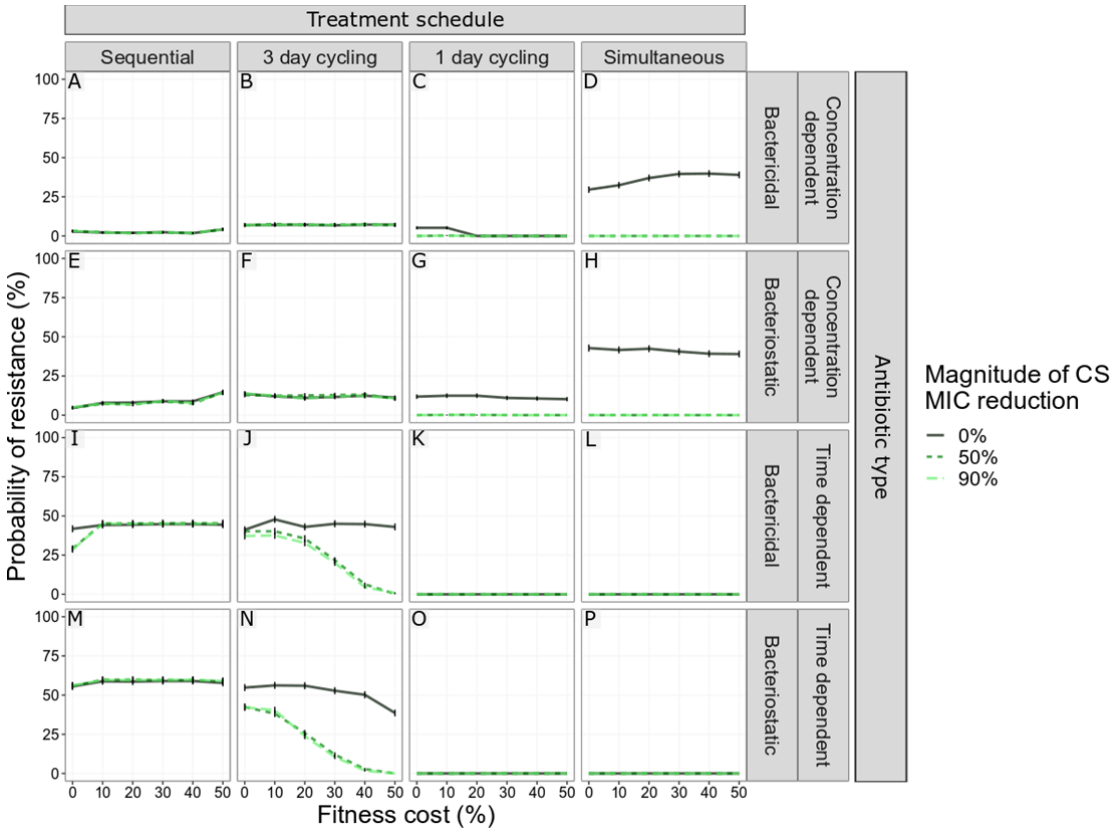

343

344 **Figure 8. The effect of fitness costs for developing resistance for different levels of collateral sensitivity effects on the probability of**

345 **resistance (PoR).** PoR of R_{Any}, defined as the presence of any resistant subpopulation, was estimated at end of treatment for treatments using

346 different designs (columns) and antibiotic types (rows). Colour and line-type indicate the magnitude of reciprocal CS simulated. The error bars

347 represent the standard error of the estimation of PoR.

348 ## CS-based simultaneous treatment designs suppress pre-existing resistance

349 The presence of a low-number pre-existing resistant cells amongst the bacterial population establishing an infection

350 is a clinically realistic scenario associated with antibiotic-treatment failure[28]. We here studied if CS-based dosing

351 schedules can be used to eradicate such a heterogeneous population **(Figure 9 and S5**). In the absence of CS, the

352 pre-existence of a subpopulation of either single mutant, resulted in higher probability of the expansion and fixation

353 of these resistant populations in the majority of the simulated treatment scenarios. As with *de novo* resistance and

354 cycling regimens, the benefit of reciprocal CS was only apparent when resistance was towards the second antibiotic

355 (subpopulation R_B). This is illustrated with the one-day cycling treatments shown in Figure 9, where all CS-based

356 treatments could supress PoR for pre-existing R_B, but for failed for all with pre-existing R_A. For three day cycling

regimens and pre-existing resistance towards the first antibiotic, CS was shown to increase the PoR for R_{AB}(**Figure S5**). In the presence of CS, all simultaneously dosed treatments were effective in fully suppressing resistance regardless of pre-existing resistance **.**

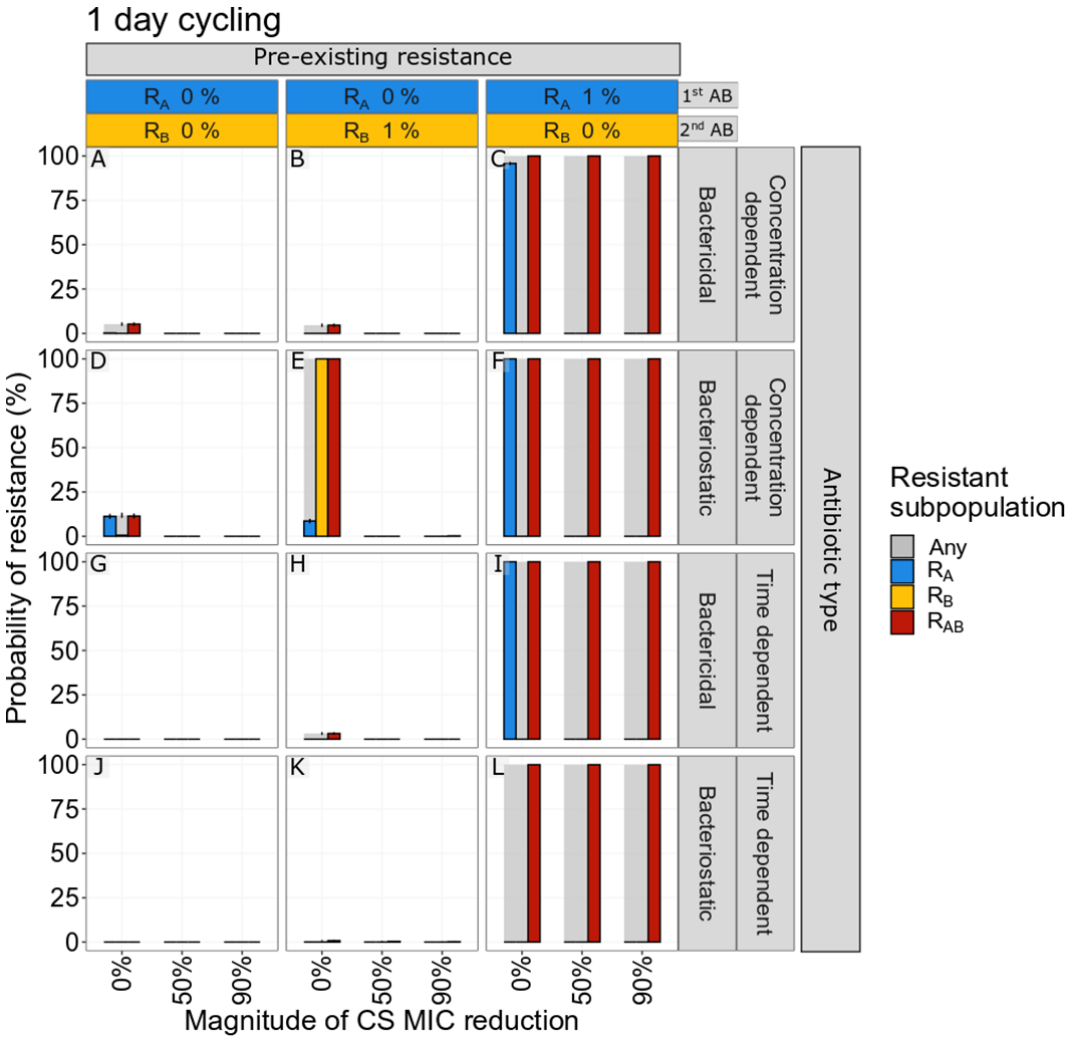

Figure 9. The effect of pre-existing resistant mutants for different magnitudes of collateral sensitivity on the probability of resistance (PoR). PoR was estimated at the end of treatment for different scenarios of low levels of pre-existing resistance (columns) and antibiotic types (rows). Subpopulation-specific probability of resistance is indicated by colour and PoR of R_{Any}, defined as the presence of any resistant subpopulation, is indicated in grey. The error bars represent the standard error of the estimation of PoR.

366 The combined effect of CS and mutation rate on resistance development differs between
367 treatments

368 Because some antibiotic treatments can enhance the genome-wide mutation rate in pathogenic bacteria [29], we
369 included a set of simulations with higher mutation rates than 10^{-9} mutations/bp/h (10^{-8}-10^{-6} mutations/bp/h). We
370 show that the impact of mutation rate on the PoR was dependent on the combination of treatment design and the
371 antibiotic type used, especially in the presence of CS (Figure 10). The largest impact of the interaction between CS
372 and mutation on PoR was found for the extremes of the time between switching of antibiotics, *i.e.,* one-day cycling
373 and sequential treatment design (maximum ΔPoR -57.8% and -52.4%, respectively). In the absence of CS, an
374 increased mutation rate generally led to an increased PoR, with the exception of simultaneous administration of
375 time-dependent antibiotics, which actually resulted in full suppression of resistance regardless of CS and mutation
376 rate for the simulated scenarios. For sequential treatments using time-dependent antibiotics with reciprocal CS
377 (Figure 10I, 10M), the highest PoR was observed at a mutation rate of 10^{-7} mutations/bp/hour, and decreased at
378 higher mutation rates. For all mutation rates and in the presence of CS, simultaneous treatments conferred
379 resistance suppression.

380

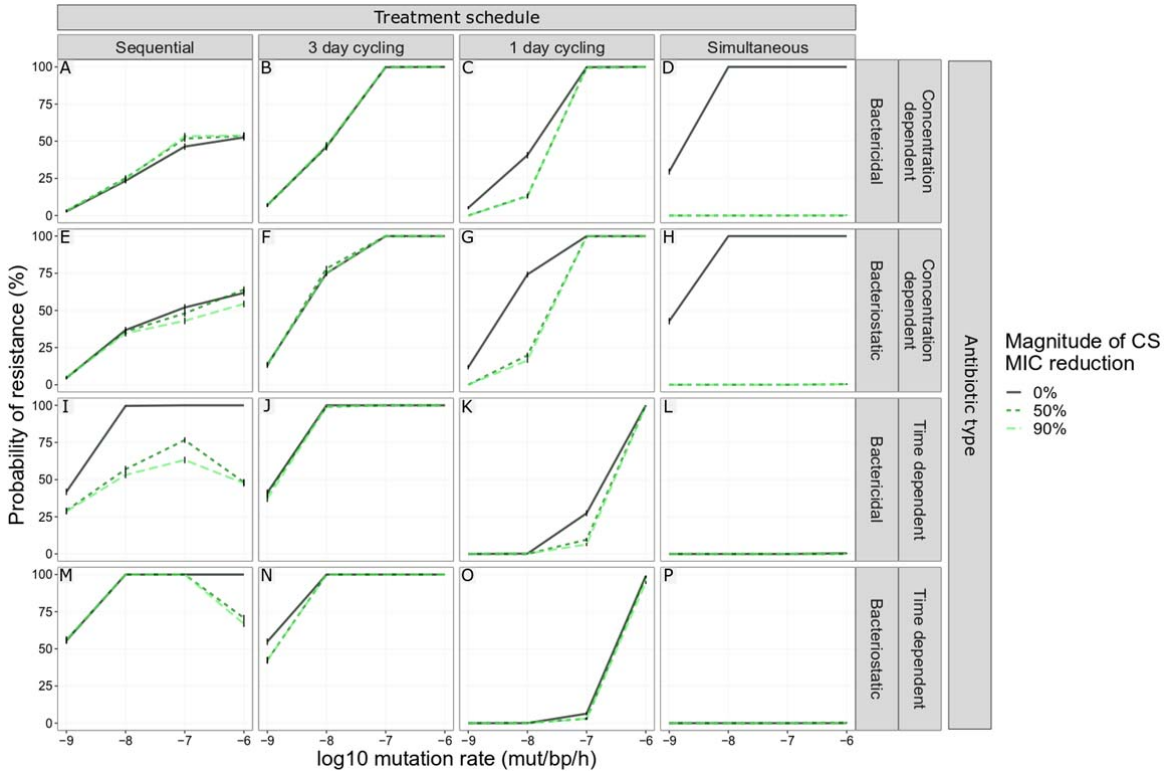

Figure 10. The effect of increased mutation rate for different CS magnitudes on the probability of resistance (PoR). The combined impact of mutation rate and the CS on PoR was dependent on treatment schedule. PoR of R_{Any}, defined as the presence of any resistant subpopulation, was estimated at the end of treatment for treatments using different designs (columns) and antibiotic types (rows) for different mutation rates (x-axis). Colour and line-type indicate the magnitude of reciprocal CS simulated. The error bars represent the standard error of the estimation.

Discussion

Our analysis shows that CS can be exploited to design treatment schedules that suppress antibiotic resistance, where CS-based treatments hold the most potential for antibiotics with narrow-therapeutic windows. Our modelling approach indicated that several factors need to be considered to ensure optimal design of CS-based dosing regimens, which include antibiotic PD characteristics, the magnitude and reciprocity of CS effects, and the effect of fitness costs, and we found that the antibiotic sequence is of importance for the success of CS-based cycling treatments.

CS-based dosing schedules have mainly considered reciprocal CS scenarios, where resistance against one antibiotic leads to increased sensitivity and vice versa[12,16]. We show, however, that one directional CS can be sufficient to supress resistance. For a one-day cycling regimen, the one-directional CS effects were nearly identical to the

398 scenario that considered reciprocal CS (**Figure 5A vs 5B**), but only when bacteria showed CS to the second drug
399 administrated. In the case where CS was only present for the first antibiotic (AB_A) (**Figure 5D**), the initial bacterial
400 growth was extensive, thus leading to increased risk of the double resistant subpopulation emerging. We consider
401 this finding relevant because one-directional CS relationships are much more common than reciprocal CS
402 relationships [9–16], thus expanding the number of clinical scenarios for which CS-based treatments can be designed.

403 We find that CS-based treatments show the greatest promise for antibiotics with narrow therapeutic window. The
404 therapeutic window of an antibiotic is defined by the drug exposure, or concentration range, leading to sufficient
405 efficacy while not leading to toxicity. In the majority of our simulations, we have studied dosing schedules leading to
406 an antibiotic steady state concentrations (C_{ss}) of 1.5xMIC, which led to full kill of the sensitive population but did
407 allow emergence of resistance to occur. This concentration can be considered to reflect a narrow-therapeutic
408 window antibiotic, *e.g.,* where the antibiotic concentration required for bacterial killing is closer to the MIC because
409 of occurrence of (severe) toxicities at higher concentrations. Indeed, for concentrations (much) higher than the MIC,
410 the benefit of CS rapidly disappears (**Figure 7**). This means that in particular for antibiotics with a narrow therapeutic
411 windows such as polymyxins or aminoglycosides, the relevance of CS-based dosing schedules is most significant.

412 Cycling based dosing regimens are frequently discussed as a strategy to utilize when CS occurs. We show that for
413 one-day cycling treatments antibiotic type (**Figure 6**), directionality of CS (**Figure 5**), and the identity of any pre-
414 existing resistance subpopulation (**Figure 9**) should be considered when choosing which drug to initiate therapy with.
415 We find that the type of the first administrated antibiotic had a larger impact on the PoR compared to the type of
416 the second administrated antibiotic, the presences of CS to the second administrated antibiotic had a greater effect
417 PoR compared to CS to the first administrated antibiotic, and the PoR was smaller if there was pre-existing resistance
418 to the second administrated drug compared to the first antibiotic. These findings are in line with previous studies
419 which show that the probability of resistance development is influenced by the sequence of antibiotics[30], and
420 optimized cycling sequences outperformed random drug cycling regimens [13]. Furthermore, in the context of cycling,
421 or alternating antibiotic treatments, consideration of the pharmacokinetics, e.g. the time-varying antibiotic
422 concentrations was found to be of importance because remaining concentration of the first antibiotic administered
423 add to the total drug effect. Therefore, the antibiotic switch contributes to a higher total drug effect than after

424 repeated administration of the same drug**.** In our simulations, the impact of this increased effect is dependent on the
425 type of the antibiotic and was shown to be especially important for time-dependent antibiotics.

426 To better characterize the population dynamics of pathogens in response to antibiotic treatment under presence of
427 CS, we studied the effect of fitness costs of antibiotic resistance and mutation rates leading to antibiotic resistance.
428 We find that the introduction of fitness cost had negligible effect on PoR for the majority of the simulated CS-based
429 treatments, with the exception of the three-day cycling using time dependent antibiotics (**Figure 8J and 8N**), where
430 the introduction of fitness cost improved the CS-based treatments because it prevents resistant bacteria to reach
431 high levels before the first antibiotic switch. Pathogens with a low mutation rate (10^{-9}), one-day cycling regimens are
432 most relevant to benefit from CS, whereas for high mutation rates (*e.g.,* 10^{-6}), sequential or simultaneous antibiotic
433 treatments are most beneficial (**Figure 10**). This means that in situations when the occurrence of hypermutator
434 strains is likely, *e.g.*, such as in CF [31], this should be considered in the design of dosing schedules. With respect to the
435 competition between different bacterial subpopulations occurring *in vivo*, we included a bacterial carrying capacity
436 which introduces clonal competition. During clonal competition, competition between subpopulations can lead to
437 their suppression, *e.g.*, high densities for one subpopulation can suppress the growth of a second subpopulation,
438 even if the second population might be more fit. When CS is present, single resistant subpopulations are unable to
439 reach high enough levels to suppress the growth of the double resistant mutant, which allows the double mutant to
440 take over, for some treatments.

441 Udekwu *et al*[32] previously demonstrated the utility of mathematical modelling to study cycling schedules for CS to
442 delay emergence of antibiotic resistance *in silico*, simulating an *in vitro* chemostat experimental system, identifying
443 the cycling interval to be the main factor impacting resistance development, and we consider this work as an
444 important foundation of our study. Our study advances the work by Udekwu by explicitly comparing treatment
445 outcomes to a base scenario without CS to determine the specific contribution of CS effects, and we perform a more
446 systematic analysis of key drug- and pathogen specific factors that could influence optimal CS-based treatment
447 scenarios.

448 Our mathematical model was designed to facilitate identification of the primary factors driving the success or failure
449 of antibiotic treatments in a general setting, and not for specific antibiotics or pathogens. We thereby did not
450 consider factors that could further contribute to treatment outcomes for specific pathogens or antibiotics. We did

451 not consider more complex evolutionary mutational trajectories can occur with associated complex patters of
452 changes in antibiotic sensitivity and MIC[33], which are not easily definable to apply to antibiotic treatment in general.
453 Other factors not considered include local antibiotic tissue concentrations [34,35], pharmacodynamic drug-drug
454 interactions or the contribution of the immune system. We expect that such factors will not affect specific
455 subpopulations studied in different ways and therefore not have a great impact on the general findings we do in this
456 analysis. The developed modelling framework is applicable for design of clinical treatment designs for specific
457 antibiotic agents and pathogens, where the model can be further expanded with additional pathogen-, drug-, and
458 patient-specific characteristics[36], derived from separate experimental studies and by utilizing published clinical
459 population PK models for specific antibiotics[37,38], which include inter-individual variability or target site
460 concentrations at the site of infection. This would thus allow to derive tailored CS-based dosing regimens for specific
461 antibiotics and pathogens.

462 We conclude that CS-based treatments are likely to be able to contribute in the suppression of resistance. However,
463 the success of such treatment strategies will be dependent on careful design of a dosing schedule, and requires
464 explicit consideration of pathogen- and drug-specific characteristics. Our developed modelling framework can be of
465 use to facilitate the design of such treatment. In addition, the robustness of such CS effects is another external factor
466 that remains a key requirement, although reciprocal CS may not be a requirement to design such dosing schedules.
467 CS treatments appear to be most relevant for antibiotics with a narrow therapeutic index, which are also the
468 antibiotics where within-host emergence of resistance is most likely to occur.

469 Acknowledgements

470 We wish to acknowledge Dr. Hadi Taghvafard for helpful mathematical input, Laura Zwep for valuable discussions,
471 and Tingjie Guo for reviewing the model code.

472 Author contributions

473

474 L.B.S.A. and J.G.C.H. designed the study; L.B.S.A. performed the data analysis; L.B.S.A., J.G.C.H., A.L., D.R. supported
475 interpretation of results; L.B.S.A., J.G.C.H., D.R., A.L., P.H.G. wrote the paper; J.G.C.H. conceived the project; All
476 authors reviewed the paper

477 # Competing interests

478 No competing interest to declare.

479 # References

480 1. Luepke, K. H. *et al.* Past, Present, and Future of Antibacterial Economics: Increasing Bacterial Resistance,
481 Limited Antibiotic Pipeline, and Societal Implications. *Pharmacotherapy* (2017). doi:10.1002/phar.1868

482 2. Mcgrath, D. M. *et al.* Genetic Basis for In Vivo Daptomycin Resistance in Enterococci. *n engl j med* **365**, 892–
483 900 (2011).

484 3. Mwangi, M. M. *et al.* Tracking the in vivo evolution of multidrug resistance in Staphylococcus aureus by
485 whole-genome sequencing. *Proc. Natl. Acad. Sci. U. S. A.* **104**, 9451–9456 (2007).

486 4. Nielsen, E. I. & Friberg, L. E. Pharmacokinetic-pharmacodynamic modeling of antibacterial drugs. *Pharmacol.*
487 *Rev.* **65**, 1053–1090 (2013).

488 5. Bonhoeffer, S., Lipsitch, M. & Levin, B. R. Evaluating treatment protocols to prevent antibiotic resistance.
489 *Proc. Natl. Acad. Sci. U. S. A.* **94**, 12106–12111 (1997).

490 6. Baym, M., Stone, L. K. & Kishony, R. Multidrug evolutionary strategies to reverse antibiotic resistance. *Science*
491 *(80-.).* **351**, aad3292–aad3292 (2016).

492 7. Imamovic, L. & Sommer, M. O. A. Use of collateral sensitivity networks to design drug cycling\nprotocols that
493 avoid resistance development. *Sci. Transl. Med.* **5**, 204ra132 (2013).

494 8. Lejla Imamovic, A. *et al.* Drug-Driven Phenotypic Convergence Supports Rational Treatment Strategies of
495 Chronic Infections. *Cell* **172**, 121–134 (2018).

496 9. Podnecky, N. L. *et al.* Conserved collateral antibiotic susceptibility networks in diverse clinical strains of
497 Escherichia coli. *Nat. Commun.* **9**, 3673 (2018).

498 10. Barbosa, C., Römhild, R., Rosenstiel, P. & Schulenburg, H. Evolutionary stability of collateral sensitivity to
499 antibiotics in the model pathogen Pseudomonas aeruginosa. *Elife* **8**, 1–22 (2019).

500 11. Gonzales, P. R. *et al.* Synergistic, collaterally sensitive β-lactam combinations suppress resistance in MRSA.
501 *Nat. Chem. Biol.* **11**, 855–861 (2015).

502 12. Imamovic, L. & Sommer, M. O. A. Use of collateral sensitivity networks to design drug cycling protocols that
503 avoid resistance development. *Sci. Transl. Med.* **5**, (2013).

504 13. Maltas, J. & Wood, K. B. Pervasive and diverse collateral sensitivity profiles inform optimal strategies to limit
505 antibiotic resistance. *PLOS Biol.* **17**, e3000515 (2019).

506 14. Barbosa, C. *et al.* Alternative Evolutionary Paths to Bacterial Antibiotic Resistance Cause Distinct Collateral
507 Effects. *Mol. Biol. Evol.* **34**, 2229–2244 (2017).

508 15. Liakopoulos, A., Aulin, L. B. S., Buffoni, M., van Hasselt, J. G. C. & Rozen, D. E. Allele-specific collateral and
509 fitness effects determine the dynamics of fluoroquinolone-resistance evolution. Preprint at
510 https://doi.org/10.1101/2020.10.19.345058 (2020).

511 16. Kim, S., Lieberman, T. D. & Kishony, R. Alternating antibiotic treatments constrain evolutionary paths to
512 multidrug resistance. *Proc. Natl. Acad. Sci.* **111**, 14494–14499 (2014).

513 17. Regoes, R. R. *et al.* Pharmacodynamic Functions: a Multiparameter Approach to the Design of Antibiotic
514 Treatment Regimens. *Antimicrob. Agents Chemother.* **48**, 3670–3676 (2004).

515 18. Coen Van Hasselt, J. G. & Iyengar, R. Systems pharmacology: Defining the interactions of drug combinations.
516 *Annu. Rev. Pharmacol. Toxicol.* **59**, 21–40 (2019).

517 19. Sharma, R. & Sharma, S. Physiology , Blood Volume. *StatPearls* **I**, 6–9 (2020).

518 20. Gerlini, A. *et al.* The Role of Host and Microbial Factors in the Pathogenesis of Pneumococcal Bacteraemia
519 Arising from a Single Bacterial Cell Bottleneck. **10**, (2014).

520 21. Martínez, J. L. & Baquero, F. Mutation Frequencies and Antibiotic Resistance. *Antimicrob. Agents Chemother.*
521 **44**, 1771–1777 (2000).

522 22. Wang, W., Hallow, K. M. & James, D. A. A Tutorial on RxODE : Simulating Differential Equation
523 Pharmacometric Models in R. 3–10 (2016). doi:10.1002/psp4.12052

524 23. Fidler M, Hallow M, Wilkins J, W. W. RxODE: Facilities for Simulating from ODE-Based Models. R package
525 version 1.0.6. (2021).

526 24. Falagas, M. E. & Kasiakou, S. K. Toxicity of polymyxins: A systematic review of the evidence from old and
527 recent studies. *Crit. Care* **10**, (2006).

528 25. Mattie, H., Craig, W. A. & Pechere, J. C. Determinants of efficacy and toxicity of aminoglycosides. *J. Antibiot.*
529 *(Tokyo).* **24**, 281–293 (1989).

530 26. Zasowski, E. J. *et al.* crossm Identification of Vancomycin Exposure-Toxicity Thresholds in Hospitalized
531 Patients Receiving Intravenous Vancomycin. *Antimicrob. Agents Chemother.* **62**, e01684-17 (2018).

532 27. Andersson, D. I. & Hughes, D. Antibiotic resistance and its cost : is it possible to reverse resistance ? *Nat. Rev.*
533 *Microbiol.* **8**, (2010).

534 28. Band, V. I. *et al.* Antibiotic failure mediated by a resistant subpopulation in Enterobacter cloacae. *Nat.*
535 *Microbiol.* **1**, 16053 (2016).

536 29. Long, H. *et al.* Antibiotic treatment enhances the genome-wide mutation rate of target cells. *PNAS.* **113**,
537 E2498-E2505 (2016).

538 30. Nichol, D. *et al.* Steering Evolution with Sequential Therapy to Prevent the Emergence of Bacterial Antibiotic
539 Resistance. *PLOS Comput. Biol.* **11**, e1004493 (2015).

540 31. Looft, C. *et al.* High Frequency of Hypermutable Pseudomonas aeruginosa in Cystic Fibrosis Lung Infection.
541 *Science.* **288**, 1251–1254 (2000).

542 32. Udekwu, K. I. & Weiss, H. Pharmacodynamic considerations of collateral sensitivity in design of antibiotic
543 treatment regimen. *Drug Des. Devel. Ther.* **12**, 2249–2257 (2018).

544 33. Aulin, L. B. S. *et al.* Distinct evolution of colistin resistance associated with experimental resistance evolution
545 models in Klebsiella pneumoniae. *J. Antimicrob. Chemother.* **76**, 533–535 (2021).

546 34. Välitalo, P. A. J. *et al.* Structure-Based Prediction of Anti-infective Drug Concentrations in the Human Lung
547 Epithelial Lining Fluid. *Pharm. Res.* ***33,*** 856–867 (2016).

548 35. Aulin, L. B. S. *et al. Pharm. Res.* **35**, 26 (2018).

549 36. Aulin, L. B. S. *et al.* Biomarker-Guided Individualization of Antibiotic Therapy. *Clin. Pharmacol. Ther.* (2021).
550 doi:10.1002/cpt.2194

551 37. Aulin, L. B. S. *et al.* Population Pharmacokinetics of Unbound and Total Teicoplanin in Critically Ill Pediatric
552 Patients. *Clin. Pharmacokinet.* **60**, 353–363 (2021).

553 38. Cock, P. A. J. G. De *et al.* Population pharmacokinetics of cefazolin before , during and after cardiopulmonary
554 bypass to optimize dosing regimens for children undergoing cardiac surgery. *J. Antimicrob. Chemother.* **72**,
555 791–800 (2017).

556 39. Pál, C., Papp, B. & Lázár, V. Collateral sensitivity of antibiotic-resistant microbes. *Trends Microbiol.* **23**, 401–
557 407 (2015).

558